Spectroscopic Evaluation of Models for Polyelectrolyte Chain Conformation in Dilute Solution

Wanda J. Walczak,* David A. Hoagland, and Shaw L. Hsu

Polymer Science and Engineering Department and Materials Research Laboratory, University of Massachusetts, Amherst, Massachusetts 01003

Received September 11, 1995[⊗]

ABSTRACT: Conformational changes of the weak polyelectrolyte poly(acrylic acid) are monitored by polarized Raman spectroscopy as a function of molecular weight and concentration when the polymer is ionized under salt-free conditions. Persistence lengths are obtained by interpreting the depolarization ratio for CH stretching in terms of the relative number of gauche and trans conformers and then inserting these conformer statistics into a simplified rotational isomeric state model. The results show that in semidilute solution, chains extend beyond persistence lengths predicted by wormlike chain models that employ the full Poisson−Boltzmann equation, irrespective of molecular weight. In dilute solution, on the other hand, the data agree best with models that adopt the Debye−Huckel approximation. Manning condensation is not followed in either concentration regime for the molecular weights studied inasmuch as the persistence length increases at ionizations above the condensation threshold. The concentration dependent intrinsic persistence length found may be attributed to the amount of cooperativity exhibited by hydrogen bonding.

Introduction

The structure of a neutral linear polymer in dilute solution can be well described by chain models incorporating only two parameters, the excluded volume and the persistence length. This success suggests that long range segment−segment interactions, as represented by the excluded volume, and short range configurational hindrances, as reflected in the persistence length, can be analyzed separately and then combined in a hybrid conformational description approximately valid over all length scales. The purpose of this investigation is to probe whether or not the same result holds true for polyelectrolyte solutions, systems in which electrostatic interactions act both locally and globally. For polyelectrolytes, the concentrations of polymer and added small ions can each control the range of electrostatic interactions, leading to a complex array of possible conformational behaviors. Our work adopts the overall strategy to compare persistence lengths obtained from a method sensitive to local chain structure with the persistence lengths predicted by electrostatic wormlike chain models. The selected measurement method, vibrational spectroscopy, probes the chain at length scales comparable to or slightly less than the persistence length; in contrast, most previous persistence length measurements extrapolated data more reflective of global chain structure. Since the experiment and theory in the present study both focus on short range behavior, chain models can be evaluated without concern for excluded volume effects.

In an earlier publication, we established that the persistence length for a salt-free, semidilute solution of poly(acrylic acid) (PAA) could be measured by depolarized Raman spectroscopy.[1] The length so obtained was compared to various polyelectrolyte wormlike chain models. Because of excessive signal-to-noise in the Raman spectra, we were unable to extend the same procedure to a dilute solution, an environment where the most accepted theory for polyelectrolyte solutions, that of Odijk, Skolnick, and Fixman, could be directly applied.[2−4] In this new contribution, we present persistence length data as a function of ionization, molecular weight, and polymer concentration for salt-free PAA. Persistence lengths for PAA from the vibrational method will be compared to those obtained by scattering and viscometric methods. The spectroscopic results will help outline the breadth and accuracy of various polyelectrolyte chain models and, in particular, the way these models incorporate electrostatic forces into the calculation of chain stiffness.

Experimental Procedures

Solutions of 2000 molecular weight PAA were prepared by dissolving 0.01−0.1 g of the solid polymer powder (Aldrich Catalog No. 32,366−7) in 1.0 mL of distilled water. The conductivity of the water was <2.5 $m\Omega^{-1}$/cm (Cole Parmer solution analyzer Model No. 5800−05 with Model No. 1481−62 gold conductivity dip cell), a level suggesting the likely presence of ions from dissolved CO_2. An XPS survey scan of a solution-cast film on glass revealed the elements Na, C, and O. Subsequent elemental analysis found 51.3% C, 6.18% H, and 0.8% Na, in comparison to 50.0% C, 6.0% H, and 0% Na expected. Dialysis of a 1.0 wt % solution against deionized water for 1 week (Spectra/Por cellulose ester membrane with molecular weight cutoff 1000) did not significantly reduce the level of unwanted Na. Ion exchange (AGMP50 resin, 100−200 mesh, hydrogen form, Bio-Rad Catalog No. 143−0841) using a batch method, however, was more successful, as evidenced by an elemental analysis revealing 51.0% C, 6.4% H, and < 0.1% Na. The batch method involved three steps: first, 10.0 g of the as-received polymer was dissolved in 100 mL of distilled methanol. Second, 5.0 g of the resin was mixed with this solution for 24 h, and lastly, the solution was filtered and freeze dried. Removal of Na by ion exchange was subsequently found to affect the Raman spectra only imperceptibly, implying that Na at trace levels does not modify local chain conformation. Due to the absence of additional counterions or other ionic species in the XPS spectrum, we believe the as-received 2000 molecular weight polyelectrolyte to be essentially salt-free.

To modify ionization, solutions were titrated with NaOH using a digital pH meter (Cole Parmer solution analyzer Model No. 5800−05 with Model No. L-05997−10 pH electrode).

* Current address: NIH, 9000 Rockville Pike, Bldg. 10/Rm. 5D14, Bethesda, MD 20892.

[⊗] Abstract published in *Advance ACS Abstracts,* October 15, 1996.

S0024-9297(95)01359-3 CCC: $12.00

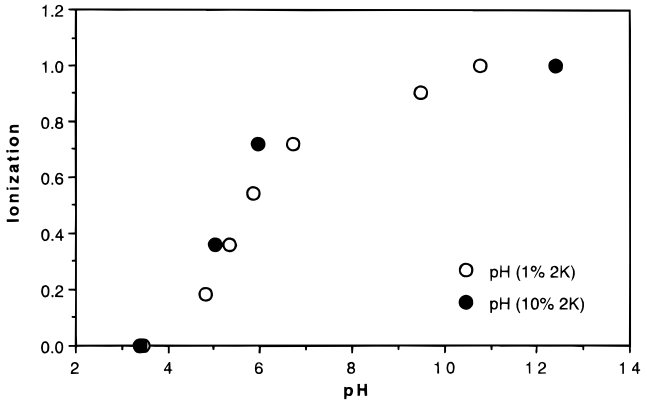

Figure 1. Poly(acrylic acid) titration curves for 2000 molecular weight solutions at 1.0 and 10.0 wt %.

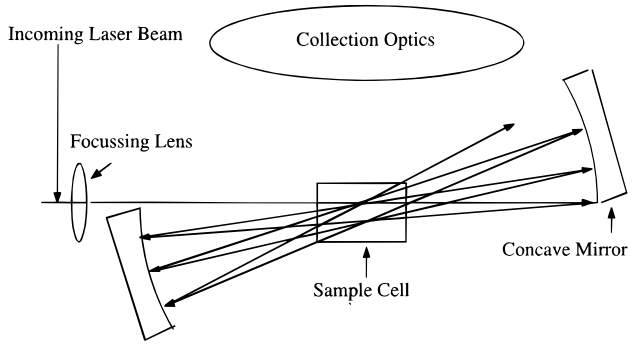

Figure 2. Multipass cell schematic.

Typical titration curves for 1.0 and 10.0 wt % PAA solutions are shown in Figure 1. Ionization I was calculated

$$I = \{-[OH^-] + [H^+] + [MOH]\}/C_p \quad (1)$$

where $[OH^-]$ and $[H^+]$ are hydroxide and hydrogen ion concentrations determined from solution pH, and [MOH] and C_p are the concentrations of the ionizing agent and polymer, respectively.[5]

A vertically polarized Spectra-Physics 165 argon ion laser tuned to the 5145 Å excitation line provided the incident intensity for the depolarized Raman experiment. A polarizer film mounted in a Newport Model RSA-2 rotation stage selectively transmitted scattered light of the appropriate linear polarization to the detection optics, and this light was then converted to circular polarization by a scrambler, ensuring that the gratings of the downstream detection system would not induce polarization artifacts. The spectra were collected by an ISA Ramanor U-1000 double monochromator operating in tandem with a photon counting photomultiplier system. Photon counts were stored and manipulated by a computer operating Spectra-Link software (Galactic Industries). Attention focused on the CH stretching region from 2850 to 3050 cm^{-1}, with intensities sampled in 0.5 cm^{-1} increments at 10 s/pt.[6] During data collection, the sample solutions were held in a 10 mm × 10 mm × 50 mm rectangular quartz cuvette positioned to maximize the scattered intensity. In initial experiments using more concentrated polymer samples, the four horizontal slits of the monochromator were opened to 300 μm, and the four vertical slits were fully opened. With this arrangement, the signal-to-noise ratio was found satisfactory for polymer solutions above about 5.0 wt %. Before scanning, samples were allowed to equilibrate in the 100 mW incident beam for ca. 12 h.

For the lower concentrations—the primary interest of the current study —poor signal-to-noise was observed even with the improved experimental procedures outlined in the previous paragraph. To enhance the signal to an acceptable level for solutions as dilute as 1.0 wt %, the multipass sample cell (SPEX Model No. 1443U external resonating cavity) shown in Figure 2 was added. This cell sharply increased the scattering volume, and thus the signal-to-noise ratio, by passing the incident beam back and forth through the sample cuvette using two opposed concave mirrors. At the same time, additional scattered light was collected by opening the four horizontal slits of the monochromator to 600 μm. For pure CCl_4, the new arrangement increased the signal-to-noise by an additional factor of about 8. Although the incident beam in the multipass cell was not exactly at 90° with respect to the collection optics, the depolarization ratio ρ for the 459 cm^{-1} band of CCl_4 was essentially unchanged from the standard 90° cell arrangement. For example, the measured ρ of CCl_4 changed from 0.0023 in the standard arrangement to 0.0034 in the multiple pass arrangement. This band is expected to be completely polarized ($\rho = 0$).[7]

Spectra were initially treated with the Savitsky−Golay smoothing option (sensitivity = 25) in the Spectra Calc program. With concentrated solutions, obvious minima on each side of the appropriate peak were hand-picked, a two-point baseline correction was performed, and the peak area was calculated. Similar handling of dilute solution data led to abnormally small persistence lengths, a trend traceable to the relatively greater influence of baseline curvature on dilute solution spectra. Thus, with dilute solutions, two fitting points were selected on either side of the polymer peak and a third-order polynomial was applied to approximate the background scattering of water. In either polymer concentration regime, duplicate measurements provided estimates of the reproducibility of the method; the reproducibility is reflected by the error bars in each figure. Inhomogeneities that produce multiple scattering have been blamed for inaccuracy in the measurement of ρ.[8] To check for multiple scattering, depolarized spectra of CCl_4 were taken with PAA solutions placed in the incident beam. If multiple scattering occurred in the PAA solution, the depolarization ratio of the CCl_4 459 cm^{-1} band would change from its expected value of zero. In fact, with a 10.0 wt % PAA solution in place, ρ of the CCl_4 459 cm^{-1} band changed only insignificantly from 0.0023 to 0.0036. Likewise, with a 1.0 wt % PAA solution placed in front of a capillary filled with CCl_4, the CCl_4 459 cm^{-1} band depolarization ratio changed from 0.0029 to 0.0035. Multiple scattering was thereby discounted as a means of error in the measurement of ρ.

We extracted conformational parameters from the Raman data using a procedure superior to the one described by us previously.[1] As before, the depolarization ratio ρ is formally defined

$$\rho = I_\perp/I_\parallel \quad (2)$$

or as the ratio of perpendicularly polarized scattered intensity to that which is parallel polarized. Equation 2 can be rewritten as the number ratio of gauche and trans isomers that exhibit perpendicular and parallel polarized scattering[9]

$$\rho = \frac{xI_{\perp g} + I_{\perp t}}{xI_{\parallel g} + I_{\parallel t}} \quad (3)$$

where x is the isomeric gauche to trans ratio, $I_{\perp g}$ and $I_{\perp t}$ are the scattered intensities for gauche and trans isomers analyzed by perpendicular polarization, respectively, and $I_{\parallel g}$ and $I_{\parallel t}$ are these intensities analyzed by parallel polarization. To relate ρ to x, one must first determine separate depolarization ratios for the gauche and trans isomers of PAA, ρ_{gauche} ($=I_{\perp g}/I_{\parallel g}$) and ρ_{trans} ($=I_{\perp t}/I_{\parallel t}$), respectively. These depolarization ratios can be written in terms of the derivative of the trace and anisotropy of each isomer's polarizability tensor, α, with respect to the normal coordinate of vibration, Q,

$$\rho = \frac{3\gamma'^2}{45\bar{\alpha}'^2 + 4\gamma'^2} \quad (4)$$

where γ' is the derivative of the anisotropy of α and $\bar{\alpha}'$ is the derivative of the trace of α, both with respect to Q.[10] Therefore,

$$\gamma'^2 = \frac{1}{2}[(\alpha'_1 - \alpha'_2)^2 + (\alpha'_3 - \alpha'_2)^2 + (\alpha'_3 - \alpha'_1)^2] \quad (5)$$

where α_1', α_2', and α_3' are the principal polarizability derivatives determined via

$$\alpha'_1 = \frac{\partial \alpha_{xx}}{\partial Q} = \frac{\partial \alpha_{xx}}{\partial r}\frac{\partial r}{\partial Q} \tag{6}$$

and

$$\bar{\alpha}' = \frac{1}{3}(\alpha'_1 + \alpha'_2 + \alpha'_3) \tag{7}$$

We employed Gough's tabulated values for gauche and trans *n*-butane as estimates for $\partial\alpha_{xx}/\partial r$, $\partial\alpha_{yy}/\partial r$, and $\partial\alpha_{zz}/\partial r$, where r is the CH stretching internal coordinate. Our earlier analysis utilized these values as if the polarizability tensor elements lay along or perpendicular to the CH bond, as used in the Wolkenstein assumption.[1,11] α_{xx} in eq 6 rather represents the polarizability tensor element in a different coordinate frame, that defined in Figure 1 of ref 11. Substitution yields ρ_g for the sum of the CH symmetric and asymmetric stretching vibrations as 0.3512 (the maximum value of this sum is 1.5 since the maximum value of an individual vibration is 0.75) and ρ_t as 0.1104.

The rest of the calculation proceeds as earlier.[1] The total intensity scattered by the gauche isomer I_g ($=I_{\perp g} + I_{\parallel g}$) is now related to that scattered by the trans isomer I_t ($=I_{\perp t} + I_{\parallel t}$). The intensity of scattered light when the incident light is plane polarized is obtained by[12]

$$I = KI_o \frac{(\nu_o - \nu)^4}{m\nu\left(1 - e\left(\frac{-h\nu}{kT}\right)\right)}[45\bar{\alpha}'^2 + 7\gamma'^2] \tag{8}$$

where K is a constant, I_o is the incident intensity, ν and ν_o are the absolute frequency of the normal vibration and incident light, respectively, and m is the reduced mass. Using the values of $\bar{\alpha}'$ and γ' for gauche and trans *n*-butane as well as the frequencies of the symmetric and asymmetric CH stretching vibrations reported by Snyder[13] for the same isomers, we find

$$0.66I_g = I_t \tag{9}$$

Equation 9 and the values for ρ_g and ρ_t calculated above allow x to be related to the measurable quantity ρ via

$$x = \frac{0.0892 - 0.8043\rho}{\rho - 0.3512} \tag{10}$$

The isomeric ratio x is related to the total persistence length L_p by assuming a rotational isomeric state model with one low-energy trans state of statistical weight 1 and two higher equal energy gauche states of statistical weight σ. The isomeric ratio

$$x = 2\sigma \tag{11}$$

where σ is defined by

$$\ln \sigma = -\Delta E/RT \tag{12}$$

Here ΔE is the energy change between gauche and trans states, R is the gas constant, and T is the temperature. The average of cos ϕ, the cosine of the dihedral angle is determined by

$$\langle \cos \phi \rangle = z^{-1}\sum u_\eta \cos \phi_\eta \tag{13}$$

where z is the partition function or the sum of statistical weights, u_η is the statistical weight of state η, and ϕ_η is the dihedral angle of that state. If the trans state where $\phi = 0$ is given a statistical weight of 1 and the two gauche states described by $\phi = \pm 120°$ are given statistical weights of σ then

$$\langle \cos \phi \rangle = (1 - \sigma)/(1 + 2\sigma) \tag{14}$$

The limiting characteristic ratio at high molecular weight, C_∞, can then be determined as

$$C_\infty = \left(\frac{1 - \cos \theta}{1 + \cos \theta}\right)\left(\frac{1 + \langle \cos \phi \rangle}{1 - \langle \cos \phi \rangle}\right) \tag{15}$$

where θ is the valence angle between bonds.[14] The total persistence length is finally obtained,

$$L_p = (L/2)(C_\infty + 1) \tag{16}$$

where L is the carbon−carbon bond length.

Data collected in our earlier publication have been reanalyzed by the new method presented above and slightly different persistence length values obtained; these reanalyzed values are presented here for comparative purposes. Uncertainties in the persistence length were determined by standard propagation of errors[15] beginning with the experimentally determined uncertainty in ρ (ca. $\pm$ 0.003).

The intrinsic persistence length of a polyelectrolyte, that part of the chain stiffness unaffected by electrostatic interactions, is generally assumed to be independent of polymer concentration. Our experiments indicate that PAA may be an exception, as the intrinsic persistence length at zero ionization was found to vary slightly with concentration. To understand this behavior, and to probe more fully the conformational implications of hydrogen bonding in this polymer system, we also examined regions of the Raman spectra sensitive to hydrogen bonds. For this purpose, unpolarized FT Raman spectra were collected in the 180° scattering geometry using the 1.06 μm incident beam from an unpolarized CVI Nd/YAG laser and a Bruker IFS 88 FTIR equipped with a FRA 106 Raman sample module. For each FT Raman spectrum, 1000 scans were taken at 4 cm^{-1} resolution with ca. 1.3 W of incident intensity; the spectrum of the solvent-filled, silvered quartz cuvette was subtracted using the Spectra Calc program. At low polymer concentrations, several polymer spectra were added to obtain a more acceptable signal-to-noise ratio.

To verify that the depolarization ratio is truly a probe of conformational change, the effect of Fermi resonance interaction was assessed. Fermi resonance can affect the measured intensity of CH stretching by borrowing intensity from an overtone or combination band of a second vibration or chemical group. We examine the effect of Fermi resonance interaction as previously,[1] by assuming that the only possibility of interaction is between the ν_{sym}(CH) stretch and an overtone of the $\delta(CH_2)$ bend at 1456 cm^{-1}. The ν_{sym} (CH) stretching vibration is most effectively isolated from other CH stretching vibrations through the generation of isotropic Raman spectra. These are calculated via[16]

$$I_{iso} = I_{\parallel} - \frac{4}{3}I_{\perp} \tag{17}$$

Results

The CH stretching region of the polarized $X(ZZ)Y$ and $X(ZX)Y$ Raman spectra for a 1.0 wt % 2000 molecular weight PAA solution is plotted in Figures 3 and 4, respectively, with ionization I as a parameter. Analogous plots for a 10.0 wt % solution are shown as Figures 5 and 6. The CH stretching region obviously consists of two or more components, including symmetric and asymmetric CH stretching vibrations and possible Fermi resonance interactions that occur between the above and overtone or combination bands. With resolution of components difficult, the area underneath the full peak is used to calculate ρ. This parameter is plotted as a function of I in Figure 7. Previously reported data[1] for a 10.0 wt % solution of 450 000 molecular weight PAA are also included in the figure; the older data correspond to a solution at semidilute conditions, while the 2000 molecular weight sample at 1.0 wt % is dilute. At 10.0 wt %, even the 2000 molecular weight solution becomes semidilute. We

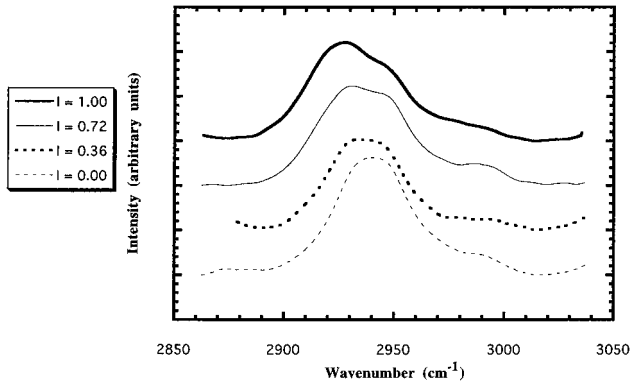

Figure 3. Baseline corrected $X(ZZ)Y$ spectra of 1.0 wt % 2000 molecular weight PAA solutions as a function of ionization, I, in the 2850−3050 cm^{-1} region. The spectra in Figures 3−6 are taken using the 5145 Å Ar^+ line and offset vertically by an arbitrary amount of intensity for clarity of display.

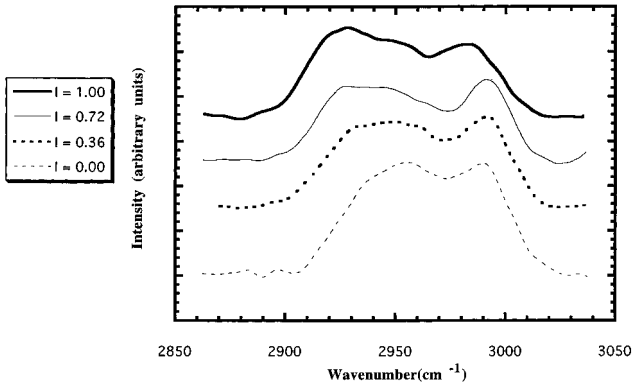

Figure 4. Baseline-corrected $X(ZX)Y$ spectra of 1.0 wt % 2000 molecular weight PAA solutions as function of ionization, I, in the 2850−3050 cm^{-1} region.

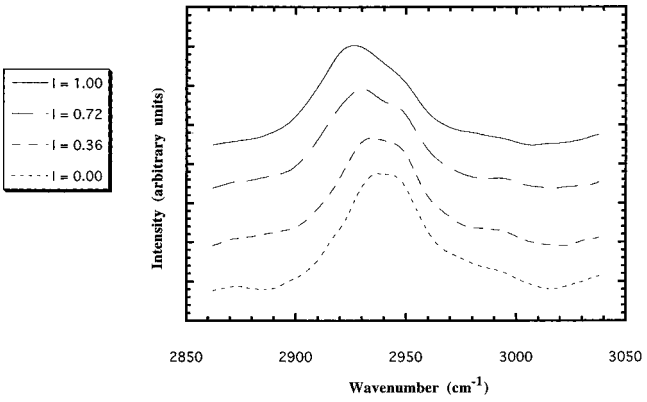

Figure 5. Baseline-corrected $X(ZZ)Y$ spectra of 10.0 wt % 2000 molecular weight PAA solutions as a function of ionization, I, in the 2850−3050 cm^{-1} region.

define a dilute solution as one where the correlation length ξ is greater than the polymer chain contour length. Odijk has modeled ξ in salt-free solution, and although his formula is far from exact, we can use the predicted value to ascertain into which concentration regime a particular solution falls:

$$\xi(c) \cong (L_{in} + L_e)^{-1/4}(\kappa)^{1/4}(Ac)^{-3.4} \qquad (18)$$

where L_{in} is the intrinsic persistence length, L_e is the electrostatic persistence length ($L_p = L_{in} + L_e$), A is the intercharge spacing, c is the monomer concentration, and κ, the inverse of the Debye−Huckel screening

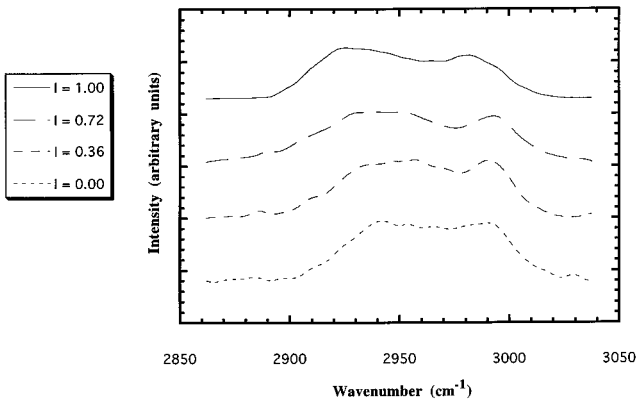

Figure 6. Baseline-corrected $X(ZX)Y$ spectra of 10.0 wt % 2000 molecular weight PAA solutions as a function of ionization, I, in the 2850−3050 cm^{-1} region.

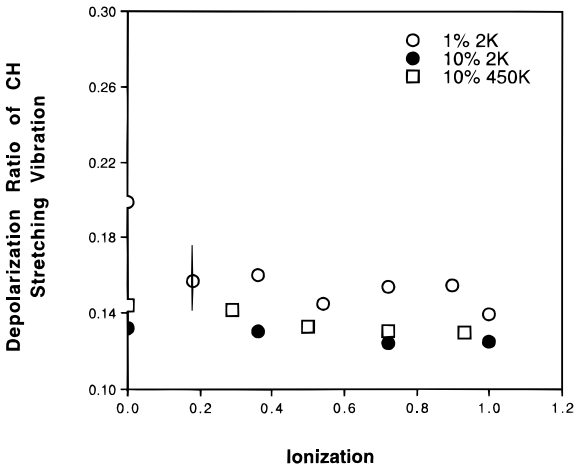

Figure 7. Depolarization ratio vs ionization for various PAA solutions. Measurement errors are within the size of the legend symbol or as indicated.

Table 1. Correlation Length for Various Polyelectrolyte Solutions Studied

C, MW	$\xi(c)$ (Å)	L (Å)
1 wt %, 2000	61.4−128	69
10 wt %, 2000	14.6−25.3	69
10 wt %, 450 000	14.4−27.4	15 625

length, is defined[17]

$$\kappa^2 = 4\pi Ac \qquad (19)$$

Values of ξ determined from experimental measurements of L_p and A are shown in Table 1. The range in correlation length tabulated is due to the range of ionization.

For all concentrations, ρ decreases with I, a trend expected if (i) more trans conformer is generated upon ionization and (ii) the trans conformer has a lower depolarization ratio than the gauche conformer. The latter expectation has been confirmed for other polymers and the model compound *n*-butane.[8,18] Using the methodology described here and in ref 1, the trans−gauche energy difference ΔE, the characteristic ratio C_∞, and the overall persistence length L_p can be calculated from ρ. Table 2 lists values compiled from all three solutions. For a 10.0 wt % solution at 2000 molecular weight, the conformer energy difference increases by ca. 14% upon full ionization: from 1850 (I = 0) to 2111 (I = 1.0) cal/mol . For comparison, ΔE increased by ca. 23% during ionization of the 450 000 sample (1567 to 1924 cal/mol). The analogous changes in C_∞ for the low and high molecular weight samples are 34.3 (unionized) to 53.8

Table 2. Conformational Analysis of Depolarized Raman Data

I	ρ	ΔE (cal/mol)	C_∞	L_p (Å)
1.0 wt % 2000 Molecular Weight PAA in water				
0.0026	0.1988	837.2	6.41	4.94
0.1806	0.1573	1341	14.5	12.0
0.3610	0.1604	1295	13.4	11.1
0.5420	0.1450	1553	20.7	16.7
0.7220	0.1542	1391	15.8	12.9
0.9020	0.1546	1384	15.6	12.8
1.000	0.1391	1678	25.6	20.5
10 wt % 2000 Molecular Weight PAA in Water				
0.000	0.1320	1850	34.33	27.2
0.361	0.1302	1905	37.72	29.8
0.722	0.1243	2124	55.06	43.2
1.000	0.1246	2111	53.80	42.2
10 wt % 450 000 Molecular Weight PAA in Water				
0	0.1438	1567	21.21	17.1
0.29	0.1418	1608	22.74	18.3
0.50	0.1332	1815	32.33	25.7
0.72	0.1303	1901	37.49	29.6
0.93	0.1296	1924	38.98	30.8

(ionized) and 21.2 (unionized) to 39.0 (ionized), respectively. Previous viscometric determinations of C_∞ for ionized PAA at θ conditions yielded values of 6.3 in dioxane and 11.3 in 1.5 M NaBr.[19,20] Takahashi et al. reported $C_\infty = 21$ for ionized PAA in 1.5 M NaBr using a light scattering method.[21]

Probably the best appreciation of ionization-induced changes in chain conformation are obtained by tracking the persistence length. For a 10.0 wt % 2000 molecular weight solution, our data show that L_p increases with ionization from 27.2 to 42.2 Å, while L_p at the same concentration for 450 000 PAA increases from 17.1 to 30.8 Å. Muroga et al. used X-ray scattering to study L_p changes for semidilute atactic PAA solutions containing added salt, finding $L_p = 8-15$ Å, independent of PAA ionization.[22] Compared to the present study, the lower persistence length and the failure to see a change of this variable with ionization could be explained by the additional electrostatic screening provided by salt. This argument does not account for the ionization invariant local conformation seen via NMR by the same authors for isotactic PAA without salt.[23] Unfortunately, the failure to report a PAA molecular weight and the different PAA tacticity makes a meaningful comparison to the present data problematical. The similarity of L_p values for the two 10.0 wt % solutions of the present study, both corresponding to semidilute solution conditions, can be traced to the strong electrostatic screening arising from a relatively high concentration of counterions.

In 1.0 wt % solutions of 2000 molecular weight PAA, conformation is a more sensitive function of I than in 10.0 wt % solutions. For example, upon full ionization, the conformer energy difference increased by ca. 200%, from 837.2 to 1678 cal/mol. The corresponding C_∞ values were 6.41 and 25.6, while L_p grew from 4.9 to 20.5 Å. The persistence lengths of the various solutions can be more easily compared after the persistence length is normalized to its intrinsic value at zero ionization, as shown in Figure 8. In 1.0 wt % 2000 molecular weight PAA, the polyion can expand freely since the correlation length at full ionization is larger than the polymer contour length. Hence, we can properly test the extensibility of fully ionized PAA.

Persistence lengths have been calculated by a method that assumes a rotational isomeric state model with a symmetric potential and posing only nearest neighbor interactions. It is widely known that an asymmetric

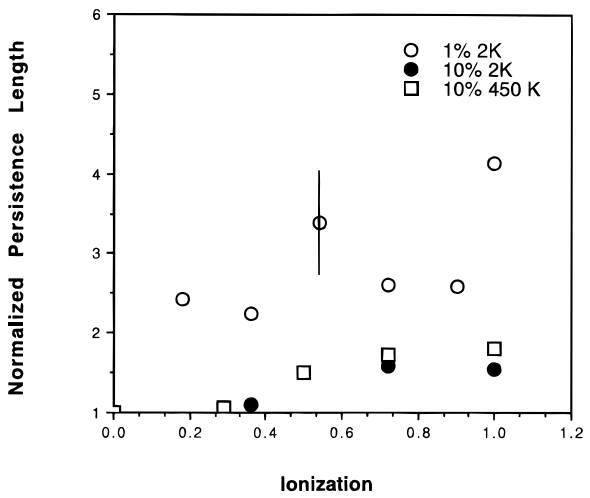

Figure 8. Total persistence length vs ionization normalized to zero ionization. Error is either the size of the symbol or as shown.

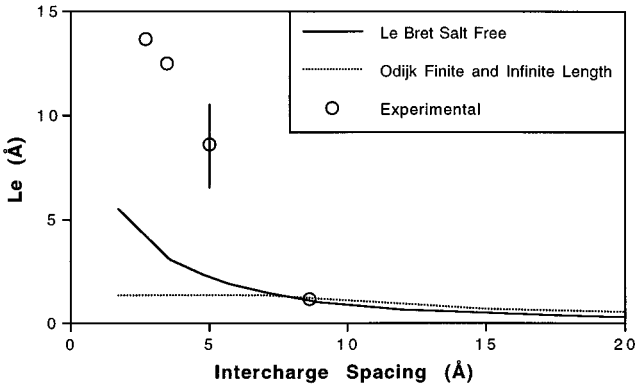

Figure 9. Comparison of experimental and theoretical persistence lengths for 10.0 wt % 450 000 molecular weight PAA in water. The Le Bret curve is for nonconducting backbones. The Odijk finite and infinite length models superimpose.

center in a vinyl polymer such as PAA complicates the rotational isomeric state analysis of the dihedral angle, perhaps rendering a symmetric potential inapplicable.[14] So too may the presence of electrostatic interactions for a charged polymer, which never fall below ca. 6 Å for the 10.0 wt % solutions and 20 Å for the 1.0 wt % solutions. It might be surprising then, to find a reasonable agreement between our C_∞ result for 10 wt % 450k PAA at zero ionization and that inferred previously by light scattering for fully ionized PAA in 1.5 M NaBr.[21] A similar and probably more surprising accord is noted between our C_∞ value for 1.0 wt % 2k PAA at zero ionization and that for fully ionized PAA at θ conditions in dioxane.[19]

Experimental persistence lengths are compared to predictions from various wormlike chain models in Figures 9−11. Odijk's model employs the linearized Poisson−Boltzmann equation to balance thermal motion with the electrostatic energy necessary to bend an infinitely long line of charge, obtaining L_e through the general relation between the bending force constant and the persistence length.[2] Skolnick and Fixman independently derived the same formula.[4] Although rigorously valid only at low charge density, it has been suggested that Odijk's model can be extrapolated to high charge densities by asserting Manning type ion condensation.[17] For a salt-free polyelectrolyte, with charge density a function of ionization, we can write $L_e \approx (16\pi Q L_m C_p)^{-1}$ for $A > Q$ and $L_e \approx (16\pi A L_m C_p)^{-1}$ for $A \leq Q$. Here, Q is the Bjerrum length, $(=e^2/\epsilon kT)$, L_m is the repeat unit

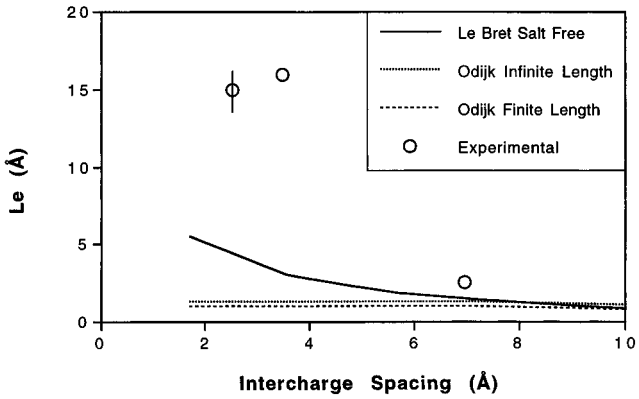

Figure 10. Comparison of experimental and theoretical persistence lengths for 10.0 wt % 2000 molecular weight PAA in water. The Le Bret curve is for nonconducting backbones.

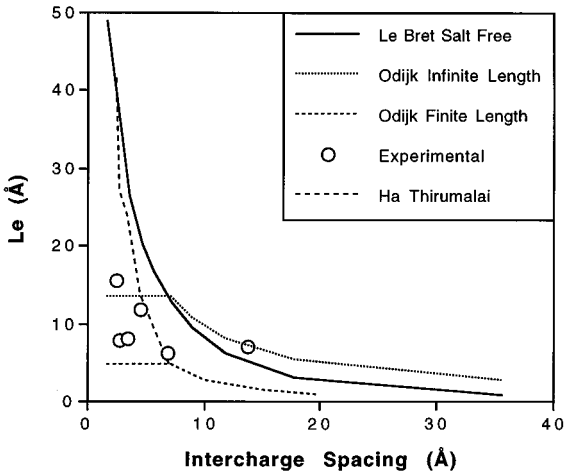

Figure 11. Comparison of experimental and theoretical persistence lengths for 1.0 wt % 2000 molecular weight PAA in water. The Le Bret curve is for nonconducting backbones. Errors are within the size of the symbol.

length, and backbone charges are separated by an average distance A ($=L_m/I$). For all cases studied, however, the persistence length was observed to vary with A, even for $A < Q$. This discrepancy between theory and experiment is rooted in the ad hoc assumption of Manning condensation when $A < Q$.

Odijk's prediction for the electrostatic persistence length is accompanied by a correction for finite chain length, and this correction becomes large when the Debye−Huckel screening length is of the order of the polymer contour length.[2] In the latter case, the persistence length falls to a fraction of its value at infinite molecular weight. While the dilute solution data of Figure 11 appear to lie between the predictions of the infinite and finite length Odijk persistence length formulas, the more general failure of Manning condensation makes a more systematic evaluation problematical.

The Odijk−Skolnick−Fixman theories have been extended to include intrinsically flexible polyions.[24−26] Ha and Thirumalai[24] predict $L_p \sim (L_{in}\omega_c)^{0.5}\kappa^{-1}$ if $L_{OSF} \gg L_{in}$. Here, $L_{OSF} = Q/4\kappa^2A^2$ and $\omega_c = Q/A^2$. This correction is applicable for our 1 wt % 2k data when $I > 0.18$ and is likewise shown in Figure 11. If Manning condensation is included, this theory coincides with Odijk's finite chain model. Polyelectrolyte stiffening beyond that determined experimentally is seen when Manning condensation is not included.

Line charge models have been improved by incorporating both nonlinear electrostatics and a finite chain radius; the inclusion of nonlinear electrostatics eliminates the need to postulate ion condensation at high ionization. We have used the salt-free persistence lengths calculated by Le Bret for chains with nonconducting backbones.[27] At 1.0 wt %, the analysis for PAA data requires an interpolation of Le Bret's tabulated values, while at 10.0 wt %, the same analysis necessitates an extrapolation. The Le Bret model agrees reasonably well with our experimental data at 10.0 wt %, but the Odijk model lies closer at 1.0 wt %. Indeed, the Le Bret model predicts almost full chain extension for 1.0 wt % 2000 molecular weight PAA, a feature clearly not shown experimentally.

To further discriminate between alternative theories, we can also analyze the persistence length as a function of monomer concentration for various intercharge spacings. Because only two polymer concentrations are available, such analysis must be viewed with caution. Assuming the power law relationship between L_e and C_p suggested by various theories, we find experimentally a power law exponent that grows from -0.37 ± 1.24 for $I = 0.36$ to -0.02 ± 0.08 for $I = 1.0$. If one models the PAA chain as having a 2 Å radius, Le Bret's nonconducting cylinder model follows $L_e \sim C_p^{-0.97}$ for $I = 0.07$ and $L_e \sim C_p^{-0.94}$ for $I = 1.0$. Odijk's theory, on the other hand, predicts $L_e \sim C_p^{-1.0}$ for all polymer concentrations. Thus, both Odijk's and Le Bret's predictions do not compare well with our limited data.

For the 10.0 wt % solutions, the correlation length does not exceed the measured persistence length. For this situation, neglect of the influence of interchain interactions on L_e, as in the theories just discussed, may seem unreasonable. Witten and Pincus and Hayter et al. presented theories that incorporate chain−chain interactions in semidilute solution, and more specifically, the effect of these interactions on chain stiffness.[28−29] Witten and Pincus assumed Manning condensation and that L_p is dominated by L_e, conditions inconsistent with our experimental results. Hayter et al. postulated that the Odijk model can be extended into semidilute solution.[2,4] Hence, Hayter's persistence length predictions do not differ from those already presented for the Odijk model.

The difference in intrinsic persistence length at the two polymer concentrations is striking. Hydrogen bonding has been postulated to affect polymer conformation due to its cooperativity.[30] One would intuitively expect that cooperative intermolecular hydrogen bonding for the unionized polymer, bridging the carbonyl moiety of one chain with the hydroxy moiety of another, would enhance chain stiffness, while intramolecular bonding of the same type would act oppositely. The relative fraction of intermolecular hydrogen bonding rises with increasing chain concentration, an effect that will lead, in the cooperative case, to larger intrinsic persistence length. This trend is experimentally observed, as the intrinsic persistence length grows from 4.9 Å for 1.0 wt % 2k PAA to 27.2 Å for a 10.0 wt % solution of the same polymer. In much the same way, the relative fraction of intramolecular hydrogen bonds diminishes as molecular weight increases at constant polymer concentration. This trend lowers the persistence length, another expectation in accord with our data: the intrinsic persistence length measured for the 10.0 wt % PAA drops from 27.2 to 17.1 Å as the molecular weight rises from 2k to 450k. According to Tanaka et al., the dimerization constant of PAA decreases with polymer concentration.[30] Unfortunately, the data used by Tanaka et al. to support this claim neither extend to polymer concentrations below 10.0 wt % nor indicate whether

intramolecular or intermolecular dimerization accounts for the decrease. Finding the carbonyl stretching region insensitive to polymer concentration below 10.0 wt %, we attempted to monitor hydrogen bonding using the more sensitive OH stretching region.[31] A downward shift in the OH stretching frequency is expected as hydrogen bonds are formed, and indeed, our experiments show that ν(OH) decreases from 3232 to 3228 cm^{-1} as the concentration of unionized PAA increases from 1.0 to 10.0%. Unfortunately, the type of hydrogen bonds affected by the concentration increase could not be identified. The only other spectroscopic manifestation of more disorder at lower concentrations is a shift in frequency of the CH stretching vibration in unpolarized FT Raman spectra. We observe a shift from 2945 to 2935 cm^{-1} as the concentration of 2k PAA increases from 1.0 to 10.0 wt %. Snyder calculated that the symmetric/asymmetric CH stretching vibrations for polyethylene increase about 6 cm^{-1} as the chains become disordered.[32] Rosenholm et al. saw similar shifts for octanoic acid as a function of concentration and used this shift to interpret order in micelle structure.[33] For small molecules, this shift was explained by a change in intramolecular force constants due to the variation in proximity between CH groups in different conformers.[34] When Na^+ replaces H^+ as the counterion during ionization, we would expect the amount of chain order arising from intermolecular OH···C═O hydrogen bonding to be suppressed.

As mentioned previously, Fermi resonance can interfere with the CH stretching bands critical to our conformational analysis and may be monitored with isotropic Raman spectra. The 10 wt % 2k isotropic spectra of PAA indicate one asymmetric peak which shifts from 2939 to 2926 cm^{-1} with increasing ionization. Similar shifts are seen for the 1 wt % 2k PAA data, where the isotropic peak shifts from 2939 to 2927 cm^{-1} with increasing ionization. As the symmetric CH stretch moves to lower wavenumber, there is an increased possibility of Fermi resonance interaction with an overtone of the $\delta(CH_2)$ bend, occurring at 1456 cm^{-1}, although we cannot distinguish a component attributable to Fermi resonance interaction in the spectra. We assume that the overtone of the $\delta(CH_2)$ bend does not shift in frequency as a function of ionization because unpolarized FT Raman data of PAA as a function of ionization show that the $\delta(CH_2)$ fundamental does not.[1] If this assumption is true, the shifts serve to lower ρ beyond that expected from conformational change alone, based on their effect on the parallel polarized spectra. On the other hand, the frequency shifts could also indicate increasing chain order, as mentioned above.

Conclusions

We have improved the Raman depolarized spectroscopy method to measure persistence length, thereby allowing measurements for dilute PAA solutions. While the persistence length in dilute solution is a more sensitive function of ionization than at higher concentration, the chain does not extend as much as predicted by Le Bret's wormlike chain model and does not follow Manning condensation. Our dilute solution data fall between Odijk's finite and infinite wormlike chain models, which employ linearized Poisson−Boltzmann electrostatics and Manning condensation. In semidilute polymer solutions, the electrostatic persistence length is greater than predicted by Le Bret. Enhanced stiffening is noted at two very different molecular weights. Moreover, an increase in polymer concentration increases the intrinsic persistence length, an unexpected phenomenon that may be explained by concentration dependent hydrogen bonding.

Acknowledgment. W.W. thanks Professor Kathy Gough for help in understanding the use of her polarizability derivatives.

References and Notes

(1) Walczak, W.; Hoagland, D.; Hsu, S. *Macromolecules* **1992**, *25*, 7317.
(2) Odijk, T. *J. Polym. Sci., Polym. Phys. Ed.* **1977**, *15*, 477.
(3) Odijk, T.; Houwaart, A. *J. Polym. Sci., Polym. Phys. Ed.* **1978**, *16*, 627.
(4) Skolnick, J.; Fixman, M. *Macromolecules* **1977**, *10*, 944.
(5) Braud, C.; Muller, G.; Fenyo, J.-C.; Selegny, E. *J. Polym. Sci., Polym. Chem. Ed.* **1974**, *12*, 2767.
(6) Bardet, L.; Cassanas-Fabre, G.; Alain, M. *J. Mol. Struct.* **1975**, *24*, 153.
(7) Brandmuller, J.; Burchardi, K.; Hacker, H.; Schrotter, H. W. *Z. Angew. Phys.* **1967**, *22*, 177.
(8) Speak, R.; Shepherd, I. W. *J. Polym. Sci. Polym. Phys. Ed.* **1975**, *13*, 997.
(9) Maxfield, J.; Shepherd, I. W. *Chem. Phys.* **1973**, *2*, 433.
(10) Steele, D. *Theory of Vibrational Spectroscopy*; W. B. Saunders Co.: Philadelphia, 1971.
(11) Gough, K. M. *J. Chem. Phys.* **1989**, *91*, 2424.
(12) Szymanski, H. *Raman Spectroscopy: Theory and Practice*; Plenum Press: New York, 1967.
(13) Snyder, R. *J. Chem. Phys.* **1967**, *47*, 1316.
(14) Flory, P. J. *Statistical Mechanics of Chain Molecules*; Wiley: New York, 1967.
(15) Peters, Dennis G.; Hayes, John M.; Hieftje, Gary M. *Chemical Separations and Measurements: The Theory and Practice of Analytical Chemistry*; W. B. Saunders Co. Philadelphia, 1974.
(16) Bogaard, M. P.; Watts, R. S. *Chem. Phys. Lett.* **1983**, *97*, 494.
(17) Odijk, T. *Macromolecules* **1979**, *12*, 688.
(18) Speak, R.; Shepherd, I. W. *J. Polym. Sci., Symp.* **1974**, *44*, 209.
(19) Newman, S.; Krigbaum, W. R.; Laugier, C.; Flory, P. J. *J. Polym. Sci.* **1954**, *14*, 451.
(20) Takahashi, A.; Nagasawa, M. *J. Am. Chem. Soc.* **1964**, *86*, 543.
(21) Takahashi, A.; Kamei, T.; Kagawa, I. *J. Chem. Soc. Jpn., Pure Chem. Sect.* **1962**, *83*, 14.
(22) Muroga, Y.; Noda, I.; Nagasawa, M. *Macromolecules* **1985**, *18*, 1576.
(23) Muroga, Y.; Noda, I.; Nagasawa, M. *J. Phys. Chem.* **1969**, *73*, 667.
(24) Ha, B.-Y.; Thirumalai, D. *Macromolecules* **1995**, *28*, 577.
(25) Barrat, J.-L.; Joanny, J.-F. *Europhys. Lett.* **1993**, *24*, 333.
(26) Li, Hao; Witten, T. A. *Macromolecules* **1995**, *28*, 5921.
(27) Le Bret, M. *J. Chem. Phys.* **1982**, *76*, 6243.
(28) Witten, T. A.; Pincus, P. *Europhys. Lett.* **1987**, *3*, 315.
(29) Hayter, J.; Janninck, G.; Brochard-Wyart, F.; de Gennes, P. G. *J. Phys. Lett.* **1980**, *41*, L451.
(30) Tanaka, N.; Kitano, H.; Ise, N. *Macromolecules* **1991**, *24*, 3017.
(31) Pimentel, G. C.; McClellan, A. L. *The Hydrogen Bond*; W. H. Freeman and Co.: London, 1960.
(32) Snyder, R. G.; Strauss, H. L.; Elliger, C. A. *J. Phys. Chem.* **1982**, *86*, 5145.
(33) Rosenholm, J. B.; Stenius, P.; Danielsson, I. *J. Colloid Interface. Sci.* **1976**, *57*, 551.
(34) Aljibury, A. L.; Snyder, R. G.; Strauss, H. L.; Raghavachari, K. *J. Chem. Phys.* **1986**, *84*, 6872.

MA951359O